Chapter 3
One-Equation Local Hyperbolic Models

3.1 Introduction

The simplest macroscopic hyperbolic models derived to investigate the movement of animal and human populations are advection and advection-reaction equations. These models describe the evolution of populations when random movement is negligible compared to directed movement. One-equation models have been employed to investigate the movement and growth of animal populations [1, 2], pedestrian and car traffic [3–7], or the formation of animal trails [8]. We mention here car traffic models, since they were the starting point for models for pedestrian dynamics. More precisely, while traffic models started being developed since the 1950s (see [3, 9]), the interest in developing models for crowd/pedestrian movement started about a decade later (see [10, 11]), being motivated by the acknowledgement of safety issues related to human traffic: evacuation of pedestrians in case of danger [12, 13], structural design of buildings, stadiums or bridges [14, 15]. We should note that more recent studies on pedestrian movement emphasised the need to consider individual social and psychological characteristics (e.g., physical and cognitive abilities, emotional condition, motivation) [16, 17] when investigating the collective movement of pedestrians. While these aspects could be easily incorporated into the kinetic theory of active particles (which will be reviewed in Chap. 6), they are not usually taken into consideration by the models investigated in this monograph.

The general advection-reaction equation that will be discussed throughout this chapter in various contexts related to animal, human, or car movement is given by:

$$\frac{\partial u}{\partial t} + H'(u)\frac{\partial u}{\partial x} = R(u), \quad u(x,0) = u_0(x). \tag{3.1}$$

Here, $u = u(x,t) : \mathbb{R} \times \mathbb{R}^+ \to \mathbb{R}$ is the population density (with $x, t \in \mathbb{R}$ and $t \geq 0$), $H(u)$ is a real nonlinear function describing the advective movement, and

R. Eftimie, *Hyperbolic and Kinetic Models for Self-organised Biological Aggregations*, Lecture Notes in Mathematics 2232,
https://doi.org/10.1007/978-3-030-02586-1_3

$R(u)$ is a real reaction term describing population growth as a result of birth and death processes. Note that the reaction term is used to model group behaviours when the movement occurs on a timescale similar or slower than the timescale of organisms growth [1, 2]. It can also model group behaviours when there is no population dynamics (i.e., no birth or death), but organisms can enter or leave a certain domain [8].

In the following we start reviewing simple models with no reaction ($R(u) = 0$). First, we present in more detail some examples of one-equation models for the evolution of the density of pedestrians/cars with different velocity functions: from constant or linear $H'(u)$ functions, to more complex multi-regime $H(u)$ functions describing different pedestrian behaviours. The traffic models in Sects. 3.2 and 3.3 are described by conservative advection equations. While the majority of examples discussed in Sects. 3.2 and 3.3 focus on single roads, we also mention briefly 1D models describing traffic on networks of roads. In Sects. 3.5 and 3.6 we review some advection-reaction models for car/pedestrian traffic and animal dynamics. In Sect. 3.7 we discuss in more detail an analytical approach used to investigate the speed of travelling wave patterns.

Remark 3.1 Before we continue with the discussion of different types of hyperbolic models for car/pedestrian traffic, we need to discuss the relevance of these continuous models at different spatial scales. The microscopic models consider the behaviour of individual cars/pedestrians under the influence of neighbouring cars/pedestrians. In these cases, the distance between cars/pedestrians is the same order of magnitude as the size of cars/pedestrians (and the spatial scale of the dynamics of the system). Note that these models could also incorporate different internal and external factors that might influence drivers/pedestrians behaviours (e.g., individual time pressure, presence of obstacles; see [18]). The mesoscopic models focus on the probability distribution of cars/pedestrians over a large spatial domain. These models investigate the impact of drivers/pedestrians attitudes and behaviours (e.g., their psychological states, or acceleration/braking and lane-changing behaviours, as given by probabilistic terms) on the overall dynamics of car/pedestrian aggregations, without distinguishing individual space-time dynamics [19]. Finally, the macroscopic models focus on the collective dynamics of cars/pedestrians, ignoring any individual behaviours. Again, the dynamics occurs on a spatial domain much larger than the magnitudes of cars/pedestrians and the distances between them. Returning to the discussion in Chap. 1 on the number of particles/cells/animals required for a mesoscopic/macroscopic model to be relevant, we note that even if the number of cars/pedestrians is usually small (e.g., in the order of tens or hundreds), continuum models have been used very often to describe the behaviours of these cars/pedestrians since existent analytical techniques can be applied to gain a better understanding of these models. It should be emphasised that there are a few studies which focus on the equivalence between microscopic models for car dynamics (in Lagrangian coordinates) and macroscopic models for the same car dynamics (in Eulerian coordinates) [20, 21]. While the fundamental diagram for the steady-state relation between speed and car density (discussed below

in Fig. 3.3a, b) is usually the same for the two classes of models, other aspects are different (e.g., the string stability condition for a second-order discrete car-following model in [20] was shown to be different from the linear stability condition of an equivalent continuum model).

3.2 First-Order Traffic Models

The advection equations discussed in Chap. 2 were initially derived in the context of car traffic [3, 4, 22], but they were later applied to pedestrian traffic [4, 23–26], or to combined car and pedestrian traffic [6]. For this reason, we briefly discuss them in the following. The generic equations are

$$\frac{\partial u}{\partial t} + \frac{\partial (uv)}{\partial x} = 0, \tag{3.2}$$

where $u = u(x,t) : \mathbb{R} \times \mathbb{R}^+ \to \mathbb{R}$ describes the density of cars or pedestrians at position x and time t, and v is their velocity. If the velocity is a constant ($v \in \mathbb{R}$), or if it is a function of time and space only ($v = v(x,t) : \mathbb{R} \times \mathbb{R}^+ \to \mathbb{R}$) or a function of density only ($v = v(u(x,t))$), then Eq. (3.2) describes an instantaneous velocity adaptation. More complicated models with non-local velocities, which take into account the velocities of other cars further away have been investigated by Helbing [4] and Helbing et al. [27]. (We will briefly return to these nonlocal models in Chaps. 5 and 6.) If $v = v(x,t)$, applying the so-called total derivative (which describes the temporal changes in a coordinate system moving with velocity v) [4],

$$\frac{d_v}{dt} = \frac{\partial}{\partial t} + v\frac{\partial}{\partial x}, \tag{3.3}$$

leads to the following form of (3.2):

$$\frac{d_v u}{dt} + u\frac{\partial v(x,t)}{\partial x} = 0. \tag{3.4}$$

Equation (3.4) says that density increases in time when the velocity decreases along the domain (i.e., $\partial v/\partial x < 0$). These models are sometimes referred to as "first-order models", being described by a transport equation for the pedestrian/vehicle density and a closed equation for the instantaneous velocity $v(u)$.

In regard to the velocity $v(u)$, these hyperbolic models generally assume that there is a speed limit v_{max}. If there are no obstacles on the road, then cars/pedestrians travel at this maximum speed: $v = v_{max}$ [4, 33]. On crowded roads, the speed is reduced. These two assumptions are incorporated into the equation for the speed as

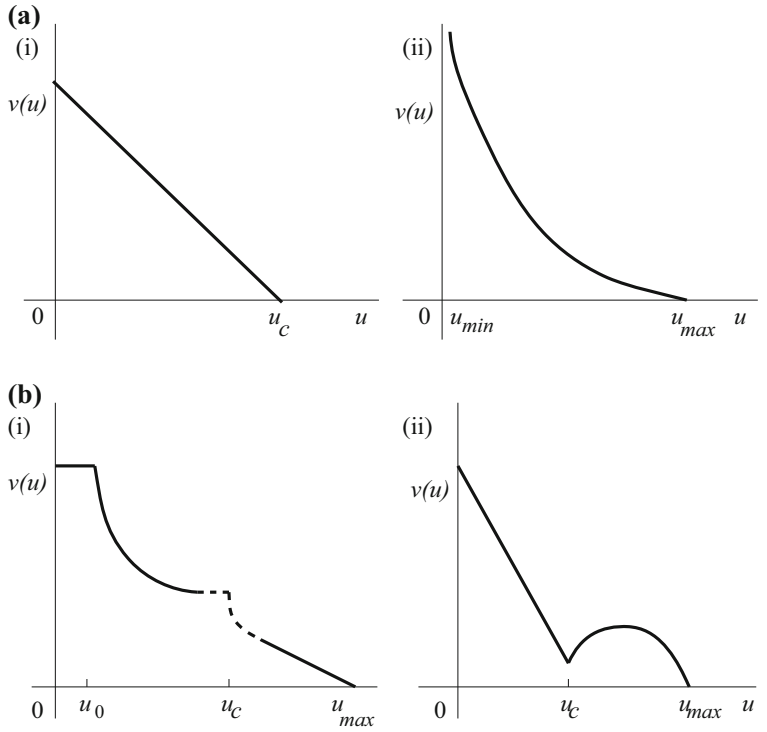

Fig. 3.1 Caricature description of various velocity functions $v(u)$. (**a**) Single stage velocities: (i) linear velocity, as introduced in [3, 28]—see also Eq. 3.5; (ii) logarithmic velocity, as given by Eq. (3.6); (**b**) Multi-stage velocity functions: (i) velocity function introduced in [29, 30]; (ii) velocity function introduced in [31]. The shape in (**b**)(ii) is consistent with experimental measurements in [32]

follows (see also Fig. 3.1a):

$$v(u) = v_{max}\big(1 - \frac{u}{u_{max}}\big), \quad \text{for } 0 \le u \le u_{max}, \tag{3.5}$$

with $u_{max} \in \mathbb{R}$ the maximum (car/pedestrian) density. A slightly different speed function, which also accounts for the slow-down at high densities is

$$v(u) = v_{max} \ln\big(\frac{u_{max}}{u}\big), \quad \text{for } u_{min} \le u \le u_{max}, \tag{3.6}$$

with $v_{max} = v^*_{max}/\ln(u_{max}/u_{min})$. Many models for traffic flow that incorporate such density-dependent speeds have been shown to exhibit shocks, which can propagate either upstream or downstream [4, 34].

While linear speeds are easier to investigate analytically, they cannot always fit observation data for pedestrian movement [14, 29, 32]. Therefore, the authors in

[14, 25] considered the following nonlinear velocity to account for the influence (on the walking velocity of pedestrians) of various physical, physiological and psychological factors represented by the geographical area and the purpose of travel (e.g., a rush hour vs. leisure time in Europe, USA or Asia):

$$v(u) = v_M\left(1 - e^{-\gamma\left(\frac{1}{u}-\frac{1}{u_M}\right)}\right). \tag{3.7}$$

Parameter γ is related to the purpose of travel, while the jam density u_M is given by $u_M = 1/(\beta_G S_m)$. Here, S_m is the mean surface occupied by a motionless pedestrian, and β_G is the coefficient for the geographical area occupied by a human body (e.g., $\beta_G = 1.075$ for European and American pedestrians, $\beta_G = 0.847$ for Asian pedestrians) [14]. Finally, v_M is the average speed, which depends on the geographic area and the purpose of travel. Note that S_m and β_G are related to the individual's repulsion area, an aspect which will be discussed again in Chap. 5 in the context of nonlocal models.

In general, for scalar conservation laws, if the initial density $u(x,0) \in [u_0^{min}, u_0^{max}]$, for all $x \in \mathbb{R}$, then the solution stays within the same bounds: $u(x,t) \in [u_0^{min}, u_0^{max}]$ for all $t \geq 0$, $x \in \mathbb{R}$ [35]. In [31] this is referred to as the maximum principle for nonlinear hyperbolic equations. However, this principle cannot account for the people behaviour in panic situations, where the maximum density increases beyond the bounds for the initial density. To address this situation, researchers have introduced models with multi-stage velocity functions (see Fig. 3.1b(ii)). For example, Colombo and Rossini [31] constructed analytically a multi-stage velocity function similar to the one described in Fig. 3.1b(ii). This particular shape of $v(u)$ is the result of certain assumptions on the flow $H(u) = uv(u)$ [36]:

- $H(u) = 0$ for $u \in \{0, u_{max}\}$;
- $H(u) \in W^{1,\infty}([0, u_{max}] \times [0, \infty)$ (finite speed of propagation of waves);
- $H(u)$ is strictly concave for $u \in [0, u_c]$ and $u \in [u_c, u_{max}]$ (to avoid mixed waves);
- maximum flow $H(u)$ calculated during panic situations (i.e., $u \in (u_c, u_{max})$ is lower than the maximum flow calculated during normal situations ($u \in (0, u_c)$);
- $H(u)$ has a local minimum at $u = u_c$, describing an increase in the flow when entering a panic regime.

Colombo and Rossini [31] focused mainly on the analytical investigation of (3.2) and showed that in addition to classical shocks and rarefaction waves (see definitions in Chap. 2), this velocity function leads to the formation of nonclassical shocks (i.e., discontinuity solutions that satisfy the Rankine-Hugoniot conditions, but not necessarily Liu's entropy condition; for details see Chapter III in [35], and our discussion of these topics in Chap. 2). Figure 3.2 shows a caricature of a nonclassical shock solution, which can describe panic situations that arise when individuals face a higher density than the one they are in. Note that this solution does not satisfy the maximum principle as defined in [31].

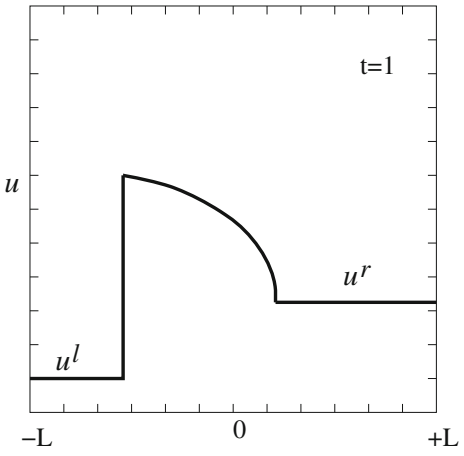

Fig. 3.2 Example of a time snapshot ($t = 1$) for a non-classical shock solution, as observed in [31], when the change in density is described by Eq. (3.2), the velocity $v(u)$ is given by a function similar to the one depicted in Fig. 3.1, and the initial condition is $u(0, x) = u^l$ for $x < 0$ and $u(0, x) = u^r$ for $x > 0$. Note that for these non-classical shocks to occur it is necessary that $u^r > u^l$

Hughes [29] also considered a multi-stage velocity function (see Fig. 3.1b) to describe a particular situation when the speed is almost constant at low densities, and concave-shaped for intermediate densities. Moreover, the velocity takes into account pedestrian discomfort that arises at very high densities. Thus, Eq. (3.2) can be modified as follows:

$$\frac{\partial u}{\partial t} + \frac{\partial}{\partial t}\left(ug(u)v^2(u)\bar{v}\right) = 0, \tag{3.8}$$

where $g(u)$ accounts for the discomfort, and the unit vector $\bar{v}$ gives the direction of movement. The simplest case would be to choose $v(u)$ as described by (3.5), and $g(u) = 1$. However, Hughes [29] chose a multi-stage velocity function (see Fig. 3.1b)

$$v(u) = \begin{cases} A, & \text{for } u < u_0, \\ A(\frac{u_0}{u})^{1/2}, & \text{for } u_0 < u \leq u_c, \\ A(\frac{u_0 u_c}{u_{max}-u_c})^{1/2}(\frac{u_{max}-u}{u})^{1/2}, & \text{for } u_c < u \leq u_{max}. \end{cases} \tag{3.9}$$

Under normal conditions, u varies between 0 and u_c. However, under exceptional panic conditions, density u can cross the threshold u_c and increase up to u_{max} (the maximum density in exceptional conditions of panic). Note that $v(u_{max}) = 0$, and thus any movement stops at very high densities. Moreover, there is a discontinuity in the gradient of the speed at $u = u_c$, which is not realistic. To model the discomfort of pedestrians in dense crowds, Hughes [29] considered

$$g(u) = \begin{cases} 1, & \text{for } u < u_c, \\ \frac{u(u_{max}-u_c)}{u_c(u_{max}-u)}, & \text{for } u_c < u < u_{max}. \end{cases} \tag{3.10}$$

Di Francesco et al. [37] considered a model similar to (3.8), with the unit vector $\bar{v}$ assumed to be parallel to the gradient of a potential $\phi(x,t)$, which describes the direction of motion of pedestrians at each point in the domain. This potential is given by the Eikonal equation

$$|\nabla\phi| = \frac{1}{v(u)}. \tag{3.11}$$

Note that the choice $v(u) = 1 - u$ can lead to a possible blow-up of $|\nabla\phi|$ when $u \to 1$, rendering the analysis very difficult. Di Francesco et al. [37] tried to address this problem by adding a small viscosity term to the Eikonal equation. They proved the existence and uniqueness of entropy solutions for the regularised equation.

A different class of transport models focus on the concept of "apparent density" felt by pedestrians, which depends on the local gradient of pedestrians' density [38].

$$u^* = u\Big(1 + \eta(1-u)\nabla u \cdot \bar{v}\Big), \tag{3.12}$$

where u^* denotes the apparent density, $\bar{v}$ is the direction vector and $\eta > 0$. If the local gradient of density is positive, then the apparent density is larger than the real density ($u^* > u$). This leads to traffic jams (associated with shocks). If, on the other hand, the local gradient is negative, then $u^* < u$. This leads to the formation of vacuum areas (associated with rarefaction waves) [14]. Although De Angelis [38] discussed possible numerical schemes to investigate the resulting models, numerical solutions were not shown, the results being mainly analytical.

The transport models (3.2) can be used to investigate the interactions between pedestrians and their environment, such as moving bridges. In this case, for example, velocity v can depend not only on the density u but also on the lateral acceleration of the bridge (z): $v = v(u,z)$ [14]. More complicated dynamics can include space dislocation (δ) and time delay (τ): $v = v(u(x+\delta,t))g(z(x,t-\tau))$. Note that these models (with space dislocation) are a particular case of nonlocal models, where the changes in velocity are given by nonlocal kernels; we will discuss nonlocal models in Chap. 5.

Many of the models described previously have been investigated in terms of existence, uniqueness and stability of solutions to the corresponding Cauchy problems (see Sect. 2.2 for a discussion of analytical approaches used to investigate these transport models). Moreover, some of those models have also been investigated in terms of optimal solutions that minimise the time of travel between two points, in the presence or absence of a time-dependent highway toll [39]. In fact, optimisation approaches are used very often in the context of car traffic on networks of roads, to choose the optimal travelling route between two points. The density-dependent speed models for traffic flow network have the general form [40, 41]:

$$\frac{du}{dt} + \frac{\partial v_{ij}(u)u}{\partial x} = 0, \tag{3.13}$$

where v_{ij} describe the nonnegative speed of cars along the arc γ_{ij} on the network (with the assumption that if two nodes, i and j, are not connected by a road then $v_{ij} = 0$). Many of these studies on flow networks focus on theoretical optimal control results, such as the minimisation of the cost incurred by different drivers with different departure and arrival times, and finding optimal and equilibrium solutions [41, 42], or the approximation of solutions of Riemann problems at the junctions [43, 44]. There are also a few studies that show numerical simulations of optimal solutions for traffic flow networks [42, 43, 45].

3.3 Second-Order Traffic Models

The models described in the previous section incorporate only the assumption that velocity changes in response to changes in pedestrian/car density. While such an assumption is not completely unrealistic [46], it does not fully describe the complexity of road and highway traffic, since velocity can also change in response to the traffic ahead (e.g., on-ramp highway situations). This leads to the so-called "second-order models": a conservation equation for the density $u \in \mathbb{R}$ of pedestrians/vehicles, coupled with a second equation for the changes in the average velocity $v \in \mathbb{R}^+$:

$$\frac{\partial u}{\partial t} + \frac{\partial (uv)}{\partial x} = 0 \tag{3.14a}$$

$$\frac{\partial v}{\partial t} + v\frac{\partial v}{\partial x} = F(u). \tag{3.14b}$$

Note that these two equations correspond to the conservation of mass and momentum, as used in continuum dynamics [47]. The term $F(u)$ describes (1) how the average velocity v adapts to an equilibrium velocity $v_e \in \mathbb{R}^+$, and (2) the drivers' (or pedestrians') awareness of the traffic conditions ahead. The simplest form of $F(u)$ includes only a velocity adaptation: e.g., $F(u) = \frac{1}{\tau}(v_e(u) - v)$, where τ is a relaxation time scale, and v_e could be a constant [48] or could depend on the car density [49]. More complex (and more realistic) terms $F(u)$ can incorporate traffic pressure $(1/u)\partial p/\partial x$, with $p = p(u)$ being the pressure, which is an increasing function of the density u: $F(u) = -\frac{1}{u}p_x + \frac{1}{\tau}(v_e - v)$ [50]. This pressure term describes preventive driving in response to road conditions [50]. In addition, $F(u)$ could also include a small viscosity component $\nu_0 \partial^2 v/\partial x^2$, which is introduced to smear out sharp shocks and to allow for a continuous description of freeway traffic flow that can exhibit stop-and-go waves [51]: e.g., $F(u) = -\frac{1}{u}p_x + \frac{1}{\tau}(\bar{v} - v) + \nu_o v_{xx}$. In terms of pattern formation, model (3.14) can exhibit shock waves, rarefaction waves and clustering [46, 50, 52, 53]. The existence of shock waves has been confirmed both analytically (via the Rankine-Hugoniot conditions) and numerically [50, 52, 53].

In the following we will discuss briefly a few examples of second-order models, by focusing on the various terms that they incorporate. For a more general review of equations describing the changes in the velocity of these models, see [20]. A first example that we focus on here is the model introduced by Payne [54], where the author proposed the following equation for the changes in vehicles speed:

$$\frac{\partial v}{\partial t} + v\frac{\partial v}{\partial x} = \frac{v_e(u) - v}{\tau} - \frac{c_0^2}{u}\frac{\partial u}{\partial x}. \tag{3.15}$$

Parameter τ is the relaxation constant for the vehicles to approach the equilibrium speed v_e, and c_0 is an "anticipation constant" (describing driver's anticipation of the traffic ahead). Investigation of the Riemann problem associated with this model showed the existence of two types of shock waves and two types of rarefaction waves; see Sect. 2.2 for a more detailed discussion of different types of analytical solutions exhibited by hyperbolic equations/systems. Numerical investigation of model (3.14a)–(3.15) confirmed these shock waves and rarefaction waves, as well as the formation of free-flow regions and formation of clusters [52, 53].

One of the drawbacks of the model in [54] is the lack of preservation of the anisotropic nature of traffic: vehicles can move against the flow, with negative speeds [55, 56]. To address this problem, Aw and Rascale [56] introduced the following equation for the changes in speed:

$$\frac{\partial(v + p(u))}{\partial t} + v\frac{\partial(v + p(u))}{\partial x} = 0, \tag{3.16}$$

with $p(u)$ a smooth increasing function of the form $p(u) = u^\gamma$, $\gamma > 0$. Analytical results showed that model (3.14a) with speed (3.16) and stepwise initial conditions (i.e., $(u(x,0), v(x,0)) = (u_l, v_l)$ for $x < 0$ and $(u(x,0), v(x,0)) = (u_r, v_r)$ for $x > 0$) can exhibit shocks, rarefaction waves and contact discontinuities. However, in contrast to the model (3.14a)+(3.15) which can exhibit negative velocities, model (3.14a)+(3.16) exhibits only non-negative velocities.

A generalisation of the model (3.14a)–(3.16) was proposed in [33] to investigate the phase transitions (i.e., jump discontinuities—see Sect. 2.2) between un-congested and congested pedestrian regions. The model is given as follows:

$$\frac{\partial u}{\partial t} + \frac{\partial(uv)}{\partial x} = 0, \tag{3.17a}$$

$$\frac{\partial(uw)}{\partial t} + \frac{\partial(uvw)}{\partial x} = 0, \tag{3.17b}$$

$$w = v + p(u), \tag{3.17c}$$

with $u(x,t) \in \mathbb{R}$ being pedestrian density, $v \in \mathbb{R}^+$ their velocity, $w(x,t) \in \mathbb{R}^+$ the desired velocity in the absence of any obstacles, and p being the offset velocity between the desired and actual velocities (where p is an increasing function of

pedestrian density). If one assumes that the desired velocity is a constant $w = V \in \mathbb{R}^+$, then the actual velocity is given by $u = V - p(u)$. This model was then generalised to incorporate congestion constraints (as controlled by parameter ϵ that appears in the correction term Q^ϵ added to pedestrian pressure):

$$\frac{\partial u^\epsilon}{\partial t} + \frac{\partial (u^\epsilon v^\epsilon)}{\partial x} = 0 \tag{3.18a}$$

$$\frac{\partial u^\epsilon w^\epsilon}{\partial t} + \frac{\partial u^\epsilon w^\epsilon v^\epsilon}{\partial x} = 0, \tag{3.18b}$$

$$w^\epsilon = v^\epsilon + p(u^\epsilon) + Q^\epsilon(u^\epsilon), \;\; Q^\epsilon(u) = \frac{\epsilon}{\left(\frac{1}{u} - \frac{1}{u^*}\right)^g}, \;\; g > 1, \tag{3.18c}$$

with $p(u)$ a convex function describing pedestrian pressure, $p(0) = 0$, $p'(0) \geq 0$ and $p(u) \to \infty$ as $u \to u^*$. The ϵ-correction term (Q^ϵ) for the background pressure p of the pedestrians is turned on when the density is close to the congestion density (i.e., $u \to u^*$). The authors investigate this perturbation problem as $\epsilon \to 0$, and show that the transition from un-congested movement ($u < u^*$) to congested movement ($u = u^*$) corresponds to a phase transition from a compressible to an incompressible flow regime [33]. The interface between congested and un-congested regions could be investigated with the help of Rankine-Hugoniot conditions. However, such an analysis was not performed in [33]. (For a brief discussion of the Rankine-Hugoniot conditions, see Sect. 2.2.)

To understand the relation between the traffic flux uv (i.e., vehicles/pedestrians per hour) and traffic density u (i.e., vehicles/pedestrians per surface area), one uses *fundamental diagrams*. The majority of traffic models in the literature that show phase transitions [3], display a fundamental diagrams similar to the one shown in Fig. 3.3a. However, empirical data similar to Fig. 3.3b suggest that the free-flow can be represented by a curve in the flow-density plane, while the congested traffic is described by a broad spreading of measurement points [57]. This led researchers to try to develop more realistic models that can exhibit two qualitatively-different behaviours [58]: (1) free vehicular traffic at low densities; (2) congested vehicular traffic at higher densities, with one more degree of freedom (thus covering a 2-dimensional domain). However, before we discuss these models in more detail, we need to mention that for pedestrian movement, the fundamental diagrams depend on the psychological status of individuals (i.e., normal versus panic conditions; see Fig. 3.3c), on various infrastructural elements (e.g., upwards/downwards stairs; see Fig. 3.3d), or on whether the flow is unidirectional or bidirectional [32, 59, 60]. Note in Fig. 3.3c that some fundamental diagrams for pedestrian movement show increased flows not only at small/intermediate densities, but also at higher densities (e.g., in panic situations), which is different from the car traffic flows.

A new class of models that investigate phase transitions in vehicular traffic were proposed by Colombo [58, 61]. These models assume that the free-flow and the congested phases are modelled by different equations defined on two different domains (corresponding to the two domains shown in Fig. 3.3b): a first-order model

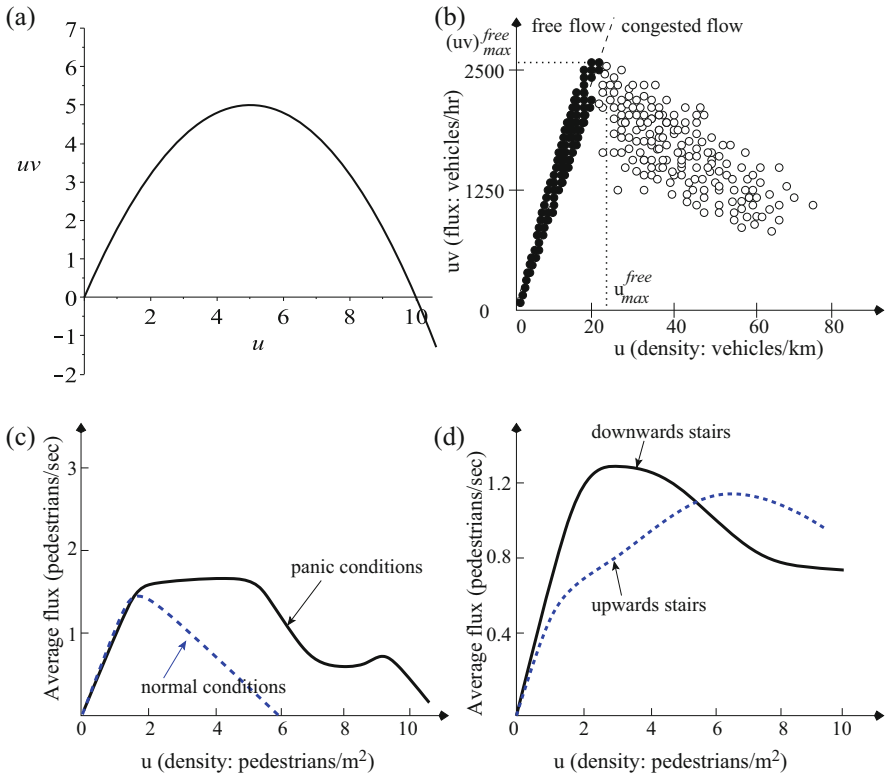

Fig. 3.3 (**a**) Fundamental traffic diagram showing traffic flux (uv) versus vehicle density (u), for the general flux function $uv_{max}(1 - u/u_{max})$; here $u_{max} = 10$, $v_{max} = 2$. (**b**) Caricature description of averaged traffic data based on real data from [57, 62–64]. As noted in [64], data in the fundamental diagram depends on the freeway location where the fundamental diagram is measured, and on the traffic demand. The diagrams show that the higher density in traffic flow corresponds to lower average vehicle speed. (**c**) Caricature description of averaged pedestrian traffic data based on real data shown in [32, 65]. The dotted blue curves approximate pedestrian movement under *normal conditions* [32, 65], while the continuous black curves approximate pedestrian movement under *panic conditions* [32]. (**d**) Caricature description of averaged pedestrian traffic data based on real data shown in [60, 66]. The dotted blue curves describe the movement on *upward stairs*, while the continuous black curves describe the movement on *downward stairs*

for the free-flow (on domain $\Omega_f \subseteq \mathbb{R}^+ \times \mathbb{R}^+$), and a second-order model for the congestion (on domain $\Omega_c \subseteq \mathbb{R}^+ \times \mathbb{R}^+$). For example, the model in [58] is described by the following equations:

$$\frac{\partial u}{\partial t} + \frac{\partial (u v_f(u))}{\partial x} = 0, \quad \text{for } (u, p) \in \Omega_f \quad \text{(free flow)}, \tag{3.19a}$$

$$\begin{cases} \frac{\partial u}{\partial t} + \frac{\partial (u v_c(u,p))}{\partial x} = 0, \\ \frac{\partial p}{\partial t} + \frac{\partial ((p-Q) v_c(u,p)}{\partial x} = 0, \end{cases} \quad \text{for } (u, p) \in \Omega_c \quad \text{(congested flow)}, \tag{3.19b}$$

with $v_f(u)$ the velocity for the free phase and $v_c(u, p)$ the velocity for the congested phase:

$$v_f(u) = \big(1 - \frac{u}{u_{max}}\big)v^*, \quad v_c(u, p) = \big(1 - \frac{u}{u_{max}}\big)\frac{p}{u}, \tag{3.20}$$

where v^* is the fee-flow speed and u_{max} is the maximum vehicle density. The variable p describes a perturbation or deviation from the equilibrium state [67]. Finally, parameter Q depends on the road conditions and characterises the phenomenon of wide traffic jams. The domains for the two phases are defined as

$$\Omega_f = \{(u, p) \in [0, u_{max}] \times [0, +\infty] | v_f(u) \geq v_f^*, q = pv^*\}, \tag{3.21a}$$

$$\Omega_c = \Big\{(u, p) \in [0, u_{max}] \times [0, +\infty] | v_c(u, p) \leq v_c^*, \frac{p - Q}{u} \in \big[\frac{Q_- - Q}{u_{max}}, \frac{Q_+ - Q}{u_{max}}\big]\Big\}, \tag{3.21b}$$

with $v_f^* < v_c^*$ two threshold speeds (above v_f^* the flow is free, below v_c^* the flow is congested). Moreover, parameters $Q_- \in (0, Q)$ and $Q_+ \in (Q, +\infty)$ depend on the environment conditions and define the width of the congested region [68]. These two phase domains are invariant, i.e., if the initial data is in the free (respectively congested) phase, then the solution stays in the free (respectively congested) phase [58]. Moreover, the solution of this model (with initial conditions $(u(x, 0), v(x, 0)) = (u_l, p_l)$ for $x < 0$, and $(u(x, 0), v(x, 0)) = (u_r, p_r)$ for $x > 0$) has been shown to be formed by phase-transition waves or rarefaction waves in Ω_f, and by shocks, contact discontinuities or rarefaction waves in Ω_c [69].

A slightly different two-phase model was proposed in [70], where the authors started with the model in [61] and assumed that $Q = 0$, while the free-flow and congestion vehicle speeds are described by:

$$v = \begin{cases} v_f(u) := v^*, & \text{for } u \in \Omega_f \\ v_c(u, p) := \big(1 - \frac{u_{max}}{u}\big)\big(a(u - u_c) + \frac{u_c v^*}{u_c - u_{max}}\big)(1 + p), & \text{for } (u, p) \in \Omega_c. \end{cases} \tag{3.22}$$

Here, u_c is a critical vehicle density (marking the transitions between the two phases), and parameter $a \in [-A, 0)$ (with $A = u_c v^*/(u_c - u_{max})^2$). See, in Fig. 3.4 two examples of congested velocities for two different values of parameter a. The Riemann problem associated with model (3.19) and speeds (3.22) (i.e., the Cauchy problem with piecewise constant initial condition $(u(x, 0), p(x, 0)) = (u_l, p_l)$ for $x < 0$ and $(u(x, 0), p(x, 0)) = (u_r, p_r)$ for $x > 0$; see also the discussion in

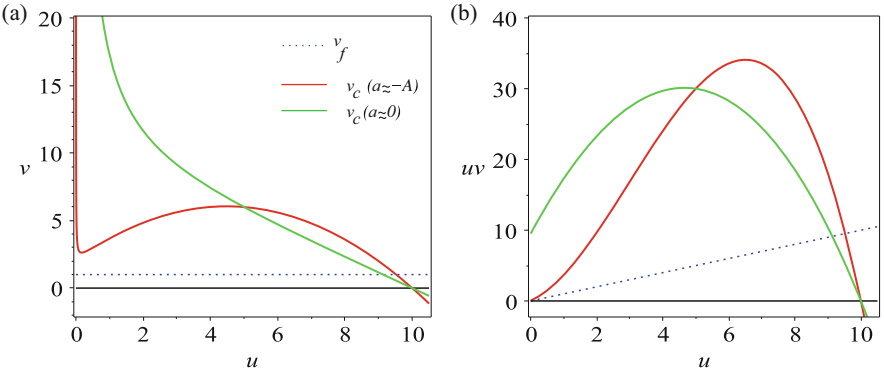

Fig. 3.4 Examples of (**a**) free-flow speed (v_f) and congested speed (v_c); (**b**) the flux function $H(u) = uv$, for the second-order traffic model (3.19)–(3.22) in [70]. The parameters are: $u_c = 5$, $u_{max} = 10$, $v^* = 0$, $A = 2$, and two values of parameter a: $a = -0.19$ (red curve), $a = -0.01$ (green curve)

Sect. 2.2) can exhibit different types of solutions when the initial conditions belong to the different phase domains [70, 71]:

- For $u_l, u_r \in \Omega_f$, the solution is represented by a contact discontinuity from u_l to u_r [71].
- For $u_l, u_r \in \Omega_c$, the solution is represented by a shock/rarefaction wave from u_l to u_m, and a 2-contact discontinuity from u_m to u_r, where u_m is the solution to the system: $p_l/u_l = p_m/u_m$, and $v_c(u_r, p_r) = v_c(u_m, p_m)$ [71].
- For $u_l \in \Omega_c$, $u_r \in \Omega_f$, the solution is represented by a 1-rarefaction wave from u_l to u_m, and a contact discontinuity from u_m to u_r [71].
- For $u_l \in \Omega_f$, $u_r \in \Omega_c$, the solution is represented by a shock from u_l to u_{m-}, and a 2-contact discontinuity from u_{m-} to u_r, where u_{m-} is the solution of the system $Q_-/u_{max} = p_{m-}/u_{m-}$ and $v_c(u_{m-}, p_{m-}) = v_c(u_r, p_r)$ [71] (Fig. 3.5).

This class of two-phase models has been further developed in other studies that used different functions for the congested speed. For example, Goatin [72] assumed that the congested speed is similar to the one in the Aw-Rascale (AR) model [56] (see Eq. (3.16)). By generalising the Aw-Rascale model to a two-phase model, the author aimed to correct some drawbacks of the original AR model, namely: lack of well-posedness near vacuum (i.e., when density is close to zero), and dependence on initial data for the maximum speed reached by vehicles on empty roads. The new two-phase model in [72] was described by the following equations:

$$\begin{cases} \frac{\partial u}{\partial t} + \frac{\partial (uv(u))}{\partial x} = 0, & \text{for } (u, v) \in \Omega_f \text{ (free flow)}, \\ v(u) := v_f(u) = \left(1 - \frac{u}{u_{max}}\right) v^* \end{cases} \tag{3.23a}$$

$$\begin{cases} \frac{\partial u}{\partial t} + \frac{\partial (uv_c(u,p))}{\partial x} = 0, & \text{for } (u, v) \in \Omega_c \text{ (congested flow)}, \\ \frac{\partial u(v+p(u))}{\partial t} + \frac{\partial (uv(v+p(u))}{\partial x} = 0, \\ p(u) = v_{ref} \ln\left(\frac{u}{u_{max}}\right). \end{cases} \tag{3.23b}$$

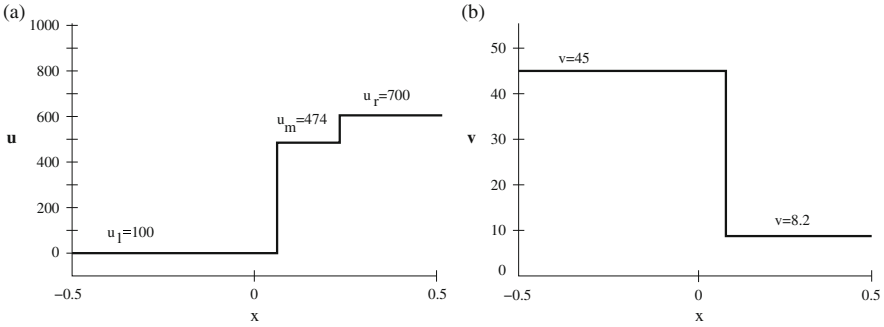

Fig. 3.5 Example of (**a**) density and (**b**) velocity profiles for a phase-transition model described in [71]. The graphs, which are re-drawn from [71], correspond to the case $u_l \in \Omega_f$, $u_r \in \Omega_c$, discussed above, where a new equilibrium state u_m appears between u_l and u_r. The parameters are: $v_* = 45$, $u_{max} = 1000$

Here, p is a pressure function related to drivers anticipation of the traffic ahead of them. The invariant domains for the free-flow and congested flow are described by:

$$\Omega_f = \{(u, v) \in [0, u^f_{max}] \times [v^*_f, v^*] | v = v_f(u)\},$$
$$\Omega_c = \{(u, v) \in [0, u_{max}] \times [0, v^*_c] | p(Q) \leq v + p(u) \leq p(u_{max})\},$$

with v^*_f and v^*_c are two threshold speeds (above v^*_f the flow is free, and below v^*_c the flow is congested; $v^* > v^*_f > v^*_c$). Parameter $Q \in (0, u_{max})$ depends on environmental conditions and determines the width of the congested region, and the maximal free-flow density u^f_{max} and reference velocity v_{ref} satisfy condition $v^*_f + v_{ref} \ln(u^f_{max}/u_{max}) = 0$. Analytical results for this model showed the existence of shocks, rarefaction waves and contact discontinuities depending on the initial data [72].

3.4 Third-Order Traffic Models

A third-order model was introduced in [73, 74], where in addition to an equation for the conservation of the density ($u \in \mathbb{R}$) and an equation for the evolution of the velocity ($v \in \mathbb{R}^+$), the model contained also an equation for the velocity variance $\theta \in \mathbb{R}^+$. To this end, Helbing [73, 74] started with the following gas-kinetic traffic model for the phase-space density of vehicles $\rho(w, t, x)$ (moving with velocity w, but having a desired velocity w_e),

$$\frac{\partial \rho}{\partial t} + \partial \rho w \partial x + \frac{\partial}{\partial w}\left(\rho \frac{dw}{dt}\right) + \frac{\partial}{\partial w_e}\left(\rho \frac{dw_e}{dt}\right) = \left(\frac{\partial \rho}{\partial t}\right)_{fluctuation} + \left(\frac{\partial \rho}{\partial t}\right)_{interaction}. \quad (3.24)$$

This equation includes (on the right-hand side) a velocity fluctuation term due to imperfect driving, and a deceleration term due to interactions between different cars. By considering the moment equations associated with this kinetic model, Helbing [73, 74] derived the following third-order traffic model for the spatial density $u(x,t) = \int \rho(w,t,x)dv$, the average velocity $v(t,x) = \int w(\rho(w,t,x)/u(t,x))dw$, and the velocity variance $\theta(t,x) = \int (w - v(t,x))^2(\rho(w,t,x)/u(t,x))dw$:

$$\frac{\partial u}{\partial t} + \frac{\partial (uv)}{\partial x} = 0, \tag{3.25a}$$

$$\frac{\partial v}{\partial t} + v\frac{\partial v}{\partial x} + \frac{1}{u}\frac{\partial (u\theta)}{\partial x} = \frac{1}{\tau}(v_e(u,v,\theta) - v), \tag{3.25b}$$

$$\frac{\partial \theta}{\partial t} + v\frac{\partial \theta}{\partial x} + 2\theta\frac{\partial v}{\partial x} = \frac{2}{\tau}(\theta_e(u,v,\theta) - \theta). \tag{3.25c}$$

Here, $v_e(u,v,\theta)$ is an equilibrium velocity (of the stationary and spatially homogeneous traffic flow), $\theta_e(u,v,\theta)$ is an equilibrium variance, and τ is the relaxation time (for the adaptation in the average velocity and average variance to the equilibrium velocity and variance). In the equation for velocity, the term $v\partial(v)/\partial x$ describes velocity changes at x caused by average vehicle motion, while the term $(1/u)(\partial u\theta)/(\partial x)$ accounts for driver's awareness of the traffic ahead [73]. (Note that the number "2" in the equation for the velocity variance arises during the calculation of the second moment $m_2 = \int dw \int w^2(w_e)\rho(w,w_e,t,x)dw_e$.)

As we have previously discussed, one of the most studied characteristics of vehicular traffic is equilibrium solutions. Since the number of vehicles is conserved, the equilibrium traffic of all these models (including model (3.25)) is uniquely determined by the averaged spatial density $\bar{u} = \int u(x,t)dx$. The equilibrium velocity and equilibrium variance can be obtained after integrating the previous equations [73]. This particular model added more realism to the literature of complex highway traffic: for small variance in speed, the cars travelled more or less at the same speed, while for large variance in the speed some vehicles travelled faster than others, causing lane changes.

3.5 Traffic Models that Include Reaction Terms

For all these different types of traffic models, reaction terms can be added to describe the rates at which pedestrians (or cars) enter or leave a particular domain (see [4, 8] and the references therein). For example, the following equation was derived by Helbing et al. [8] to describe the movement of pedestrians belonging to a subpopulation u_a (part of the whole population u):

$$\frac{\partial u_a}{\partial t} + \frac{\partial (u_a v(x,t))}{\partial x} = R_a^+(x,t) - R_a^-(x,t). \tag{3.26}$$

Here, $R_a^{\pm}(x,t)$ are the rates at which pedestrians join and leave sub-population u_a. (In the context of car traffic, $R^{\pm}(x,t)$ usually denote the inflow/outflow of cars on ramps.) In [8], this reaction-advection equation was then coupled with an equation for the environmental changes (i.e., trail formation) caused by these pedestrians:

$$\frac{dG}{dt} = G_0(x) - G(x,t) + \left(1 - \frac{G(x,t)}{G_{max}(x)}\right) \sum_a K(x) u_a(x,t). \tag{3.27}$$

Here G is a ground potential that measures the comfort of walking (with G_{max} the maximum clearing of the trail from vegetation), $G_0(x)$ describes the existent trails (at positions x), and $K(x)$ measures the attractiveness of the trail (at different spatial positions x). Numerical simulations showed the formation of a simple trail system (i.e., network patterns; see also Fig. 1.11), the shape of which depended on the magnitude of K.

Models for pedestrian traffic (with pedestrians entering/leaving the domain) exhibit various types of human behaviours, depending on the density of individuals [4]. For example, at low densities the pedestrian flow is similar to streamlines of fluids, while at higher densities the pedestrians organise themselves into different lines of uniform walking direction [24]. Similar to car traffic, pedestrian traffic can lead as well to jams [24]. When the rates $R_{\pm}(u)$ are nonzero, models (3.26) can also exhibit patterns with increasing amplitude, such as localised clusters and stop-and-go waves (which are sequences of traffic jams that alternate with free traffic) [75]. Other pedestrian models (of Langevin type) can incorporate social interactions as well as boundary forces [23]. In particular, these models assume that pedestrians are attracted/repelled by other persons or by boundary objects (e.g., buildings). In Chap. 5, we will discuss in more detail the importance of these social interactions to the formation of various group patterns.

As we have previously seen in Sect. 3.3, reaction terms can be also added to second-order traffic models, to describe highway entries and exits, or local changes in traffic flow caused by inhomogeneities in the road. The simplest and probably one of most widely-used reaction terms is the relaxation velocity shown in Eq. (3.15). In the following we discuss the more general model introduced in [76], which incorporates different reaction terms with different physical meanings:

$$\frac{\partial u}{\partial t} + \frac{\partial u v(u,p)}{\partial x} = s_u(t,x,u,p), \tag{3.28a}$$

$$\frac{\partial p}{\partial t} + \frac{\partial (p-Q) v(u,p)}{\partial x} = s_p(t,x,u,p), \tag{3.28b}$$

with the velocity $v(u, p) = (1 - u/u_{max})(p/u)$. The explicit form of the source functions depends on the assumptions being modelled:

- vehicles entries and exits along an interval $[a, b]$ [76]:

$$s_u(t, x, u, p) = a_{in}(t, x)\big(1 - \frac{u}{u_{max}}\big) - a_{out}(t, x)\frac{u}{u_{max}},$$
$$s_p(t, x, u, p) = -\Big(\frac{a_{in}(t, x)}{u_{max}} + \frac{a_{out}(t, x)}{u_{max}}\Big)(p - Q).$$

  Here, $a_{in}(t, x) = g_{in}(t)\chi_{[a,b]}(x)$ and $a_{out}(t, x) = g_{out}(t)\chi_{[a,b]}(x)$, with $g_{in}(t)$ and $g_{out}(t)$ the fraction of the traffic density (per unit time) that enters and exits the road, respectively. The source term s_p describes a "stabilising" effect caused by the entries and exits on vehicle flow [76].
- relaxation term added to the second equation, to model acceleration towards an equilibrium velocity $v_e(u)$ [27, 76]:

$$s_u(t, x, u, p) = a(t, x)\big(1 - \frac{u}{u_{max}}\big),$$
$$s_p(t, x, u, p) = -\frac{a(t, x)}{u_{max}}(p - Q) + \frac{u_{max}}{u_{max} - u}\frac{u(v_e - v)}{\tau}.$$

  with τ the relaxation time corresponding to the average acceleration time. This can be a constant, or can be density-dependent ($\tau = \tau(u)$).
- local changes in traffic speed (while the total vehicle density is conserved) [76]:

$$s_u(t, x, u, p) = 0,$$
$$s_p(t, x, u, p) = \chi(x)ua(t, u, p),$$

  where $\chi(x)$ gives the location of a descent along the highway (between some points x_1 and x_2), and $a(t, u, p) \geq 0$ is the mean acceleration.

For more examples of source terms see [76] and the references therein. The general model (3.28) has been shown to be well posed (for suitable conditions on the source terms), thus admitting a unique solution defined for all $t > 0$ [76]. In contrast to models without a source, these models have been shown to capture the formation of queues (e.g., as for $s_u = 0$ and $s_p(t, x, u, p) = \chi(x)ua(t, u, p)$ in [76]). In this case, the increase in vehicle speed (triggered by a decrease in density associated with the exit) leads to an accumulation of vehicles into a wide moving traffic jam.

Remark 3.2 The positive and negative aspects of different traffic models have been discussed in various studies (see, for example, [55, 77, 78]), and thus we will not review them here. However, we would like to emphasise that the continuous development of all these different traffic models was triggered by the lack of realistic patterns exhibited by some earlier models. For example, since many of first-order models assumed that the average speed (v) was in equilibrium with the density

(u), they could not describe non-equilibrium situations taking place at on-ramps, or stop-and-go traffic (where the speed changes). Therefore, second-order models were introduced to add a new dynamic equation for the average velocity v. Even some of these models do not always describe the self-organised phenomena of stop-and-go waves when the density increases above a critical value [54], which lead to further refining of models [79, 80].

We will return to traffic models in Chap. 4, when we will discuss not only the patterns generated by multiple populations of car drivers/pedestrians, but also the patterns generated by ants moving along pheromone trails, and the application of systems of hyperbolic equations to the traffic of molecules along filaments.

3.6 Advection-Reaction Equations for Animal Population Dynamics

In the context of animal population growth and movement, the most common types of reaction terms $R(u)$ that appear in the general advection equation:

$$\frac{\partial u}{\partial t} + h(u)\frac{\partial u}{\partial x} = R(u), \tag{3.29}$$

are [81]:

1. quadratic (logistic) growth: $R(u) = ru(1-u)$;
2. cubic growth ("Allee" effect): $R(u) = ru(1-u)(u-\alpha)$, with $\alpha \in (0, 1)$.

Mickens [1] used a simpler version of (3.1), with constant velocity ($h(u) = 1$) and logistic growth ($R(u) = r_1 u(1 - r_2 u)$), to describe the dynamics of a generic population u. Because of the simplicity of this model, it was possible to find exact time-dependent and time-independent solutions. The time-independent solutions (i.e., the stationary solutions) were shown to be either bounded or unbounded, depending on the initial condition. Another type of solution discussed by Mickens [1] was the travelling front solution (see Fig. 3.6b). Again, because of the simplicity of the model it was possible to find an exact expression for these travelling fronts.

A slightly more complex model was investigated by Lika and Hallam [2]. When the advective velocity was described by a linear term $h(u) = -ku$ (and the growth was logistic), model (2.4) could exhibit shock solutions (see Fig. 3.6a). In particular, advective waves with low speed were shown to steepen and lead to shock formation. Note that these patterns are very common in large human aggregations which result in panic stampede. The model in [2] can also exhibit travelling front patterns (see Fig. 3.6b). These solutions, which exist only for speeds $c > 1$, are stable to certain semi-finite domain perturbations. These authors also showed that it is not possible to have travelling front patterns when the initial conditions have compact support. This is in contrast with the classical Fisher's equation, where initial conditions with

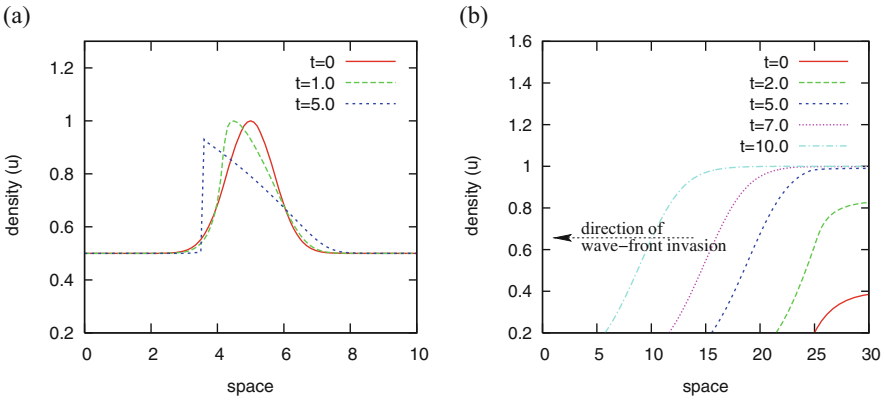

Fig. 3.6 (**a**) Shock patterns exhibited by the advection model (3.2) with density-dependent speeds $v = u(1-u)$. The initial condition is $u(0) = 0.5 + 0.5e^{-(x-5)^2}$. (**b**) Travelling front patterns exhibited by the advection reaction model (2.4), with $h(u) = u$, and $f(u) = u(1-u)$. The initial data is similar to the data used by Lika and Hallam [2]: if $x \leq x_0$ then $u(0) = 0.2e^{0.5(x-x_0)}$, and if $x > x_0$ then $u(0) = 0.2(2 - e^{-0.5(x-x_0)})$. We take $x_0 = 5L/6$, where $L = 30$ is the domain length

compact support lead to travelling front solutions moving with the minimum speed c (where $c = 2$) [82]. In Sect. 3.7, we will discuss in more detail the approach to find the speed and shape of travelling-wave solutions.

To reproduce the intricate animal population dynamics during self-organised behaviours, the models derived in the recent years contain more complex assumptions—such as nonlocal attractive-repulsive velocities [83]. We will discuss these models in more detail in Chap. 5, where we will also show the numerical patterns displayed by them.

We conclude this section by observing that some hyperbolic models consider the change of the population with respect to age $a \in \mathbb{R}^+$ (and not necessarily with respect to space x). The classical example is represented by the McKendrick–Von Foerster equation [84, 85]:

$$\frac{\partial u}{\partial t} + \frac{\partial u}{\partial a} = -\mu(a)u(a,t), \quad a > 0. \tag{3.30}$$

Here $\mu(a) \in \mathbb{R}^+$ represents the age-dependent death rate of population $u \in \mathbb{R}$. Therefore, this equation models the changes in a population as a result of becoming older and eventually dying. If $\mu(a) = 0$ then population change is only the result of getting older. The birth of the population is usually incorporated into the initial conditions:

$$u(0,t) = \int_0^\infty b(a)u(a,t)da, \quad t > 0, \tag{3.31}$$

where $b(a) \in \mathbb{R}^+$ is the birth rate for age a. The problem is completed by the specification of the initial age distribution: $u(a,0) = u_0(a)$. This equation can be solved exactly along the characteristic lines to obtain a closed-form solution [86, 87]:

$$u(a,t) = \begin{cases} u(0,t-a)e^{-\int_0^a \mu(s)ds}, & \text{when } a < t, \\ u_0(a-t)e^{-\int_{a-t}^a \mu(s)ds}, & \text{when } a \geq t. \end{cases} \tag{3.32}$$

Note that these models could also include changes in population size with respect to the space variable x:

$$\frac{\partial u}{\partial t} + \frac{\partial u}{\partial a} + \frac{\partial u}{\partial x} = -\mu(a)u(a,t). \tag{3.33}$$

A slightly different type of age-structured model with local birth terms will be presented at the end of Sect. 4.6.

3.7 Analytical Approaches for the Investigation of Patterns: Speed of Travelling Waves

Since the travelling wave solutions are one of the simplest (but biologically very important) solutions exhibited by the transport models for collective movement of animals (as well as models for car/pedestrian movement), in the following we present briefly the analytical approaches used to calculate the propagating speed and shape of these solutions for a simple 1-equation hyperbolic model introduced in Lika and Hallam [2]. For a more detailed discussion of travelling waves (and their propagation speeds) in various biological populations we refer the reader to [88–90] (although all these studies focus on parabolic equations).

Lika and Hallam [2] investigated the existence and stability of travelling wave solutions for the following (non-dimensionalised) advection-reaction model describing the movement and growth of a population with density $u(x,t)$:

$$\frac{\partial u}{\partial t} - u\frac{\partial u}{\partial x} = u(1-u). \tag{3.34}$$

Travelling wave solutions for Eq. (3.34) are nonnegative functions $0 \leq u(x,t) \leq 1$ (which connect the two spatially homogeneous steady states $u = 0$ and $u = 1$). Writing $u(x,t) = w(z)$, with $z = x + ct$ the travel-wave coordinate and $c > 0$ the wave speed to be determined, leads to the following differential equation

$$(c-w)\frac{dw}{dz} = w(1-w), \tag{3.35}$$

together with the boundary conditions

$$\lim_{z\to-\infty} w(z) = 0, \quad \lim_{z\to+\infty} w(z) = 1. \tag{3.36}$$

The travelling wave solution should also satisfy $\frac{dw}{dz} > 0$. By linearising Eq. (3.35) about the steady states $w = 0$ and $w = 1$, one obtains that the trivial state $w = 0$ is unstable for all $c > 0$ while the state $w = 1$ is stable for $c > 1$ and unstable for $0 < c < 1$.

To investigate whether it is possible to have travelling waves with speeds $c < 1$ or $c > 1$, the authors integrate Eq. (3.35) to obtain a closed-form solution:

$$\ln\left(\frac{w^c}{(1-w)^{c-1}}\right) = z + C^*, \quad C^* = const. \tag{3.37}$$

Due to the invariance of the travelling wave solution to any shift in the origin of the coordinate system, one can assume that for $z = 0$ one has $w = 1/2$, and thus the solution is $\ln(2w^c/(1-w)^{c-1}) = z$. Moreover, the steepness of the wave at $z = 0$ is $\frac{dw(0)}{dz} = 1/(4c-2)$, suggesting that the wave steepness decreases as the speed c increases; see also Fig. 3.7a.

The boundary conditions (3.36) are then used to determine the existence/absence of travelling wave solutions. For example, the boundary condition at $z = -\infty$ is satisfied by solution of (3.37) for any $c > 0$ and any constant C^*. In contrast, the boundary condition at $z = +\infty$ is (1) satisfied by the solution of (3.37) for any constant C^* when $c > 1$; (2) not satisfied by the solution of (3.37) for any constant C^* when $c < 1$. The authors in [2] conclude that for any $c > 1$ there is a travelling wave $u(x,t) = w_c(x + ct)$ that satisfies $0 \le w \le 1$ and $w(0) = 1/2$, while for

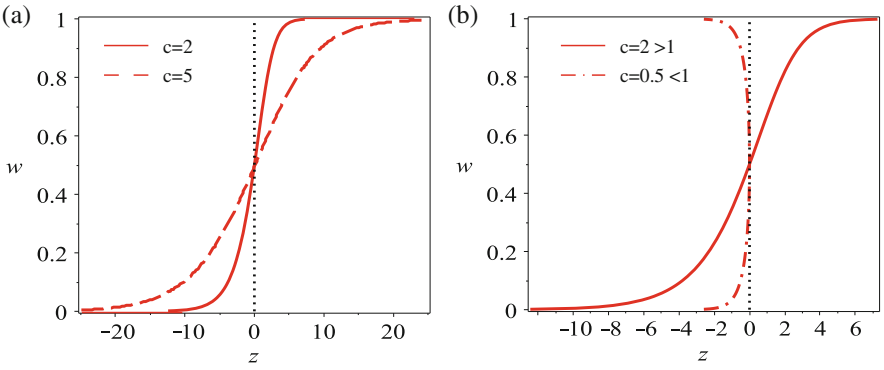

Fig. 3.7 (**a**) Description of two possible travelling wave profiles, as given by Eq. (3.37) with $C^* = 0$, for two speed values: $c = 2$ and $c = 5$. Note that lower speed is associated with a very steep profile. (**b**) Comparison between the solution of (3.37) with $C^* = 0$, when the speed $c = 0.5 < 1$ (and no travel front exists) and $c = 2 > 1$ (and a travel front exists)

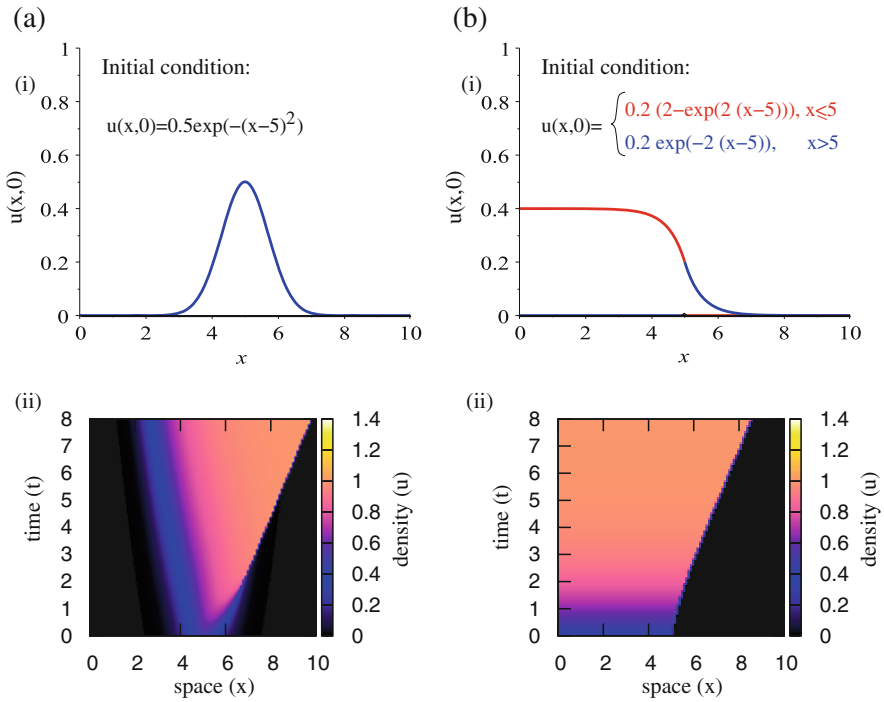

Fig. 3.8 (i) Initial density profile and (ii) spatio-temporal patterns for Eq. (3.34) when considering two types of initial conditions: (**a**) $u(x,0) = 0.5\exp(-(x-5)^2)$, and (**b**) $u(x,0) = 0.2 * (2 - \exp(2 * (x-5)))$ for $x \leq 5$ and $u(x,0) = 0.2\exp(-2(x-5))$. The simulations are performed on a finite domain $[0, L] = [0, 10]$ with: (**a**) periodic boundary conditions, and (**b**) no-flux boundary conditions.

$c \leq 1$ there is no such solution; see also Fig. 3.7b. (From (3.37) note that for $c = 1$, $w(z)$ is increasing exponentially and reaches the threshold $w = 1$ at some finite z.)

Figure 3.8 shows the numerically-simulated travelling wave/front solutions for two different types of initial conditions:

(a) a Gaussian-like function $u(x,0) = 0.5e^{-(x-5)^2}$;
(b) a composite function, as in [2]:

$$u(x,0) = \begin{cases} 0.2(2 - e^{2(x-5)}), & x \leq 5, \\ 0.2e^{-2(x-5)}, & x > 5. \end{cases} \tag{3.38}$$

Note that the logistic proliferation of population u leads to the spread of the front (in Fig. 3.8a(ii) the spread can occur both ahead and behind the initial aggregation), which adds to the transport of the population to the right, via the advection term.

Lika and Hallam [2] also investigated the stability of the travelling front to small semi-finite domain perturbations. The authors have re-written $u(x,t) = y(z,t)$ with

$z = x + ct$, and then added a small perturbation v to the travel wave solutions $w_c(z)$ (i.e., $y(z,t) = w_c(z) + v(z,t)$) and investigated when the perturbations decayed towards 0. The perturbations were defined on a semi-domain as $v(z,t) = 0$ for $z \in (-\infty, a)$ with some $a \in \mathbb{R}$. For more details, we refer the reader to [2].

Remark 3.3 We need to emphasise that for parabolic PDEs, the existence and stability of travelling front solutions is proven rigorously with the help of a classical comparison argument based on upper and lower solutions; see [91, 92]. Since for hyperbolic PDEs a similar comparison principle does not hold (see [93]), proving the existence and uniqueness of such travelling waves/fronts for kinetic transport equations (even 1-population models) is more complicated, and is not the aim of this study. Nevertheless, we need to emphasise here that all these theoretical aspects are still open problems for the great majority of the local and nonlocal kinetic and hyperbolic models presented throughout this monograph (as the majority of hyperbolic/kinetic models that investigate the travelling wave/front patterns focus mainly on the speed at which the front of the population wave invades new territories).

3.8 Numerical Approaches

For numerical simulations of these local models, one can use various numerical schemes: from first order dissipative finite difference upwind and Lax-Friedrichs schemes, to second-order dispersive finite-difference Lax-Wendroff and MacCormack schemes, and even finite volume schemes (e.g., Godunov, Roe or Engquist-Osher schemes). To minimise the dispersion that appears in second-order schemes, various flux limiters (minmod, superbee, monotonized central—MC) are used. A more detailed discussion of these numerical schemes can be found in LeVeque [47, 94]. For hyperbolic models describing traffic on networks, in the past the focus was mainly on first-order or second-order numerical schemes [95], although more recent studies have started to focus on the construction of higher order finite volume schemes [96, 97]. For an overall discussion of these various numerical schemes (and other numerical schemes derived to discretise kinetic models), see Chap. 7. Note that these numerical schemes can be applied also to systems of local and nonlocal equations (described in Chaps. 4 and 5), and for this reason in the next two chapters we will not discuss again these numerical approaches.

Regarding the specific model discussed in Sect. 3.7, the numerical simulations shown in Fig. 3.8 were obtained by discretising the transport equation using a second order MacCormack finite difference scheme (which includes also the reaction terms). The same MacCormack scheme was used to create the travelling wave and shock profiles shown in Fig. 3.6.

References

1. R. Mickens, SIAM Rev. **30**(4), 629 (1988)
2. K. Lika, T. Hallam, J. Math. Biol. **38**, 346 (1999)
3. M. Lighthill, G. Whitham, Proc. R. Soc. Lond. Ser. A. **229**(1178), 317 (1955)
4. D. Helbing, Rev. Mod. Phys. **73**, 1067 (2001)
5. D. Helbing, P. Monar, I. Farkas, K. Bolay, Environ. Plann. B. Plann. Des. **28**, 361 (2001)
6. R. Borsche, A. Meurer, Discret. Contin. Dyn. Syst. Ser. S **7**(3), 363 (2014)
7. S. Göttlich, C. Harter, Netw. Heterog. Media **11**(3), 447 (2016)
8. D. Helbing, F. Schweitzer, J. Keltsch, P. Molnar, Phys. Rev. E **56**, 2527 (1997)
9. I. Prigogine, R. Herman, *Kinetic Theory of Vehicular Traffic* (Elsevier, New York, 1971)
10. L. Henderson, Nature **229**, 381 (1971)
11. L. Henderson, Transp. Res. **8**, 509 (1975)
12. R. Colombo, M. Garavello, M. Lécureux-Mercier, Math. Models Methods Appl. Sci. **22**(4), 1150023 (2012)
13. D. Yanagisawa, A. Kimura, R. Nishi, A. Tomoeda, K. Nishinari, Distrib. Auton. Robot. Syst. **8**, 227 (2009)
14. F. Venuti, L. Bruno, Phys. Life Rev. **6**(3), 176 (2009)
15. F. Venuti, L. Bruno, Eng. Struct. **56**, 95 (2013)
16. C. Schäfer, R. Zinke, L. Künzer, G. Hofinger, R. Koch, Transp. Res. Proc. **2**, 636 (2014)
17. A. Sieben, J. Schumann, A. Seyfried, PLoS ONE **12**(6), e0177328 (2017)
18. S. Hoogendoorn, P. Bovy, Transp. Res. Board **1710**, 28 (2000)
19. S. Hoogendoorn, P. Bovy, Proc. Inst. Mech. Eng. Pt. I J. Syst. Control Eng. **215**(4), 283 (2001)
20. W. Jin, Transp. Res. B Methodol. **93**(A), 543 (2016)
21. R. Abeyaratne, Int. J. Mech. Eng. Educ. **42**(3), 185 (2014)
22. B. Piccoli, M. Garavello, *Traffic Flow on Networks* (American Institute of Mathematical Sciences, San Jose, 2006)
23. D. Helbing, P. Molnar, Phys. Rev. E **51**(5), 4282 (1995)
24. D. Helbing, Complex Syst. **6**, 391 (1992)
25. F. Venuti, L. Bruno, N. Bellomo, Math. Comput. Model. **45**(3–4), 252 (2007)
26. N. Bellomo, C. Dogbé, Math. Models Methods Appl. Sci. **18**, 1317 (2008)
27. D. Helbing, A. Hennecke, V. Shvetsov, M. Treiber, Math. Comput. Model. **35**(5–6), 517 (2002)
28. P. Richards, Oper. Res. **4**, 42 (1956)
29. R. Hughes, Transp. Res. B **36**, 507 (2002)
30. R. Hughes, Annu. Rev. Fluid Mech. **35**, 169 (2003)
31. R. Colombo, M. Rosini, Math. Method Appl. Sci. **28**(13), 1553 (2005)
32. D. Helbing, A. Johansson, H.Z. Al-Abideen, Phys. Rev. E **75**, 046109 (2007)
33. C. Appert-Rolland, P. Degond, S. Motch, Netw. Heterog. Media **6**(3), 351 (2011)
34. G. Schütz, Exactly solvable models for many-body systems far from equilibrium, in *Phase Transitions and Critical Phenomena*, vol. 19 (Academic Press, London, 2001), pp. 1–251
35. P. Lefloch, *Hyperbolic Systems of Conservation Laws. The Theory of Classical and Nonclassical Shock Waves*. Lectures in Mathematics. ETH Zürich (Birkhäuser, Basel, 2002)
36. R. Colombo, P. Goatin, M. Rosini, GAKUTO Int. Ser. Math. Sci. Appl. **32**, 255 (2010)
37. M.D. Francesco, P. Markowich, J.F. Pietschmann, M.T. Wolfram, Math. Models Methods Appl. Sci. **250**(3), 1334 (2011)
38. E.D. Angelis, Math. Comput. Model. **29**, 83 (1999)
39. A. Bressan, K. Han, SIAM J. Math. Anal. **43**, 2384–2417 (2011)
40. G. Coclite, B. Piccoli, SIAM J. Math. Anal. **36**(6), 1862 (2005)
41. A. Bressan, K. Han, Netw. Heterog. Media **8**, 627 (2013)
42. M. Herty, S. Moutari, M. Rascale, Netw. Heterog. Media **1**(2), 275 (2006)
43. G. Bretti, R. Natalini, B. Piccoli, Netw. Heterog. Media **1**(1), 57 (2006)
44. A. Bressan, S. Canić, M. Garavello, M. Herty, B. Piccoli, EMS Surv. Math. Sci. **1**, 47 (2014)
45. M. Gugat, M. Herty, A. Klar, G. Leugering, J. Optim. Theory Appl. **126**(3), 589 (2005)

46. D. Helbing, Phys. Rev. E **53**, 2366 (1996)
47. R. LeVeque, *Numerical Methods for Conservation Laws* (Birkhäuser, Basel, 1992)
48. P. Ross, Transp. Res. **22**(6), 421 (1988)
49. W. Phillips, Transp. Plan. Technol. **5**(3), 131 (1979)
50. M. Flynn, A. Kasimov, J.C. Nave, R. Rosales, B. Seibold, Phys. Rev. E **79**(5), 056113 (2009)
51. R. Kühne, M. Rödiger, *Proceedings of the 1991 Winter Simulation Conference* (1991), pp. 762–770
52. W. Jin, H. Zhang, Solving the Payne-Whitham traffic flow model as a hyperbolic system of conservation laws with relaxation. Technical report, University of California, Davis, 2001
53. A. Delis, I. Nikolos, M. Papageorgiou, Transp. Res. C.: Emerg. Technol. **44**, 318 (2014)
54. H. Payne, *Mathematical Models of Public Systems*, vol. 28 (Simulation Council, La Jolla, 1971), pp. 51–61
55. C. Daganzo, Transp. Res. B **28**, 35 (1995)
56. A. Aw, M. Rascale, SIAM J. Appl. Math. **60**, 916 (2000)
57. B. Kerner, Math. Comput. Model. **35**, 481–508 (2002)
58. R. Colombo, P. Goatin, Flow Turbul. Combust. **76**(4), 383 (2006)
59. F. Navin, R. Wheeler, Traffic Eng. **39**, 31 (1969)
60. L. Vanumu, K. Rao, G. Tiwari, Eur. Transp. Res. Rev. **9**, 49 (2017)
61. R. Colombo, SIAM J. Appl. Math. **63**, 708 (2003)
62. B.S. Kerner, P. Konhäuser, Phys. Rev. E **50**, 54 (1994)
63. B. Kerner, Phys. A: Stat. Mech. Appl. **333**, 379 (2004)
64. B. Kerner, arXiv prerint cond-mat/0309018 (2003)
65. A. Seyfried, B. Steffen, W. Klingsch, M. Boltes, J. Stat. Mech. **2005**(10), P10002 (2005)
66. V. Predtechenskii, A. Milinskii, *Planning for Foot Traffic Flow in Buildings* (Amerind Publishing, New Delhi, 1978). Translation of: Proekttirovanie Zhdanii s Uchetom Organizatsii Dvizheniya Lyuddskikh Potokov. Stroiizdat Publishers, Moscow
67. B. Piccoli, K. Han, T. Friesz, T. Yao, J. Tang, Transp. Res. C **52**, 32 (2015)
68. R. Colombo, P. Goatin, B. Piccoli, J. Hyperbolic Differ. Equ. **7**(1), 85 (2010)
69. M. Garavello, B. Piccoli, Netw. Heterog. Media **4**(1), 107 (2009)
70. S. Blandin, P. Goatin, B. Piccoli, A. Bayen, D. Work, Proc. Soc. Behav. Sci. **54**, 302 (2012)
71. S. Blandin, D. Work, P. Goatin, B. Piccoli, A. Bayen, SIAM J. Appl. Math. **71**(1), 107 (2011)
72. P. Goatin, Math. Comput. Model. **44**(3–4), 287 (2006)
73. D. Helbing, Phys. A **219**, 375 (1995)
74. D. Helbing, in *A Perspective Look at Nonlinear Media*, ed. by J. Parisi, S. Müller, W. Zimmermann. Lecture Notes in Physics, vol. 503 (Springer, Berlin, 1998), pp. 122–139
75. M. Schönhof, D. Helbing, Transp. Sci. **41**(2), 135 (2007)
76. P. Bagnerini, R. Colombo, A. Corli, Math. Comput. Model. **44**(9–10), 917 (2006)
77. J.P. Lebacque, J.B. Lesort, *Proceedings of the 14th International Symposium on Transportation and Traffic Theory, Jerusalem* (1999)
78. J.B. Lesort, E. Bourrel, V. Henn, *Proceedings of Traffic and Granular Flow?03, Delft* (2003), pp. 125–139
79. T. Li, Phys. D: Nonlinear Phenom. **207**(1–2), 41 (2005)
80. H. Yeo, A. Skabardonis, *Proceedings of the 18th International Symposium on Transportation and Traffic Theory, Hong-Kong* (2009), pp. 99–115
81. K. Hadeler, Reaction transport systems in biological modelling, in *Mathematics Inspired by Biology*. Lecture Notes in Mathematics (Springer, Berlin, 1999), pp. 95–150
82. A. Kolmogorov, I. Petrovsky, N. Piscounov, Mosc. Univ. Bull. Math. **1**, 1 (1937)
83. K. Fellner, G. Raoul, Math. Models Methods Appl. Sci. **20**, 2267 (2010)
84. A. McKendrick, Proc. Edinb. Math. Soc. **44**, 98 (1926)
85. H.V. Foerster, *The Kinetics of Cell Proliferation* (Grune and Stratton, New York, 1959), pp. 382–407
86. G. Webb, *Theory of Nonlinear Age-Dependent Population Dynamics* (Marcel Dekker, New York, 1985)
87. B. Keyfitz, N. Keyfitz, Math. Comput. Model. **26**(6), 1–9 (1997)

88. J.D. Murray, *Mathematical Biology* (Springer, New York, 1989)
89. A. Volpert, V. Volpert, V. Volpert, *Travelling Wave Solutions of Parabolic Systems* (American Mathematical Society, Providence, 2000)
90. V. Volpert, S. Petrovskii, Phys. Life Rev. **6**, 267 (2009)
91. P. Fife, J. Diff. Equ. **40**, 168 (1981)
92. P. Fife, J. McLeod, Arch. Ration. Mech. Anal. **65**(4), 335 (1977)
93. A. Bressan, *Hyperbolic Systems of Conservation Laws. The One-Dimensional Cauchy Problem* (Oxford University Press, Oxford, 2000)
94. R. LeVeque, *Finite Volume Methods for Hyperbolic Problems* (Cambridge University Press, Cambridge, 2002)
95. G. Bretti, R. Natalini, B. Piccoli, J. Comput. Appl. Math. **210**, 71 (2007)
96. R. Borsche, J. Kall, J. Comput. Phys. **327**, 678 (2016)
97. Y. Shi, Y. Guo, Appl. Numer. Math. **108**, 21 (2016)